Brown Adipose Tissue is Associated with Improved Cardiometabolic Health and Regulates Blood Pressure

Tobias Becher[1,9,10], Srikanth Palanisamy[1,2], Daniel J. Kramer[1,2,3], Sarah J. Marx[1], Andreas G. Wibmer[4], Ilaria Del Gaudio[5,11], Scott D. Butler[6], Caroline S. Jiang[7], Roger Vaughan[2,7], Heiko Schöder[4], Annarita Di Lorenzo[5], Allyn Mark[8] and Paul Cohen[1*]

[1] Laboratory of Molecular Metabolism, The Rockefeller University, New York, NY

[2] Weill Cornell Medicine, New York, NY

[3] Weill Cornell/ Rockefeller/ Sloan Kettering Tri-Institutional MD-PhD Program, New York, NY

[4] Department of Radiology, Memorial Sloan Kettering Cancer Center, New York, NY

[5] Department of Pathology and Laboratory Medicine, Cardiovascular Research Institute and Feil Brain and Mind research Institute, Weill Cornell Medicine, New York, NY

[6] Department of Biomedical Sciences, College of Veterinary Medicine, Cornell University, Ithaca, NY

[7] Center for Clinical and Translational Science, The Rockefeller University, New York

[8] Department of Internal Medicine, Carver College of Medicine, University of Iowa, Iowa City, Iowa

[9] DZHK (German Centre for Cardiovascular Research), Partner Site Heidelberg/Mannheim, Mannheim, Germany

[10] First Department of Medicine (Division of Cardiology), University Medical Center Mannheim, Mannheim, Germany

[11] Department of Obstetrics and Gynecology, Medical University of Graz, Graz, Austria

Corresponding Author:

Paul Cohen, M.D., Ph.D.

E-Mail: pcohen@rockefeller.edu

The Rockefeller University

Laboratory of Molecular Metabolism

1230 York Avenue, P.O. Box 223, New York, NY 10065

Abstract

White fat stores excess energy, while brown and beige fat dissipate energy as heat[1]. These thermogenic adipose tissues markedly improve glucose and lipid homeostasis in mouse models, though the extent to which brown adipose tissue (BAT) influences metabolic and cardiovascular disease in humans is unclear[2,3,4]. Here, we categorized 139,224 ^{18}F-FDG PET/CT scans from 53,475 patients by presence or absence of BAT and used propensity score matching to assemble a study cohort. Individuals with BAT showed lower prevalences of cardiometabolic diseases. Additionally, BAT independently correlated with lower odds of type II diabetes, coronary artery disease and congestive heart failure. These findings were supported by improved glucose, triglyceride and high-density lipoprotein values. The effects of BAT were more pronounced in overweight and obesity, indicating that BAT can offset the deleterious effects of obesity. Strikingly, we also found lower rates of hypertension among patients with BAT. Studies in a mouse model with genetic ablation of beige fat demonstrated elevated blood pressure due to increased sensitivity to angiotensin II in peripheral resistance arteries. In addition to highlighting a role for BAT in promoting overall cardiometabolic health, this study reveals a new link between thermogenic adipose tissue and blood pressure regulation.

50 **Main**

51 As early as 2003, reports described increased uptake of the labeled glucose analogue
52 ^{18}F-fluorodeoxyglucose (^{18}F-FDG) on positron emission tomography (PET) in areas
53 corresponding to supraclavicular fat on computed tomography (CT), suggesting the presence of
54 metabolically-active BAT in adult humans[5,6]. This tissue has received intense interest from the
55 biomedical community since 2009 when a series of papers confirmed the presence of active
56 BAT in adults, which correlated with lower body mass index (BMI), decreased age, colder
57 outdoor temperature, and female sex, as well as an association with decreased fasting glucose
58 levels[7,8,9,10,11,12]. Since then, small prospective studies in healthy humans have demonstrated
59 that cold-activated BAT is associated with increased whole body energy expenditure and
60 increased disposal of glucose and free fatty acids[13,14,15]. Although these properties have
61 generated great enthusiasm for BAT as a therapeutic target for obesity and its associated
62 diseases, these studies have been too small to definitively address whether brown fat is a
63 clinically meaningful modulator of metabolic and cardiovascular disease in humans.

64 To answer this central question, we reviewed 139,224 ^{18}F-FDG PET/CT reports
65 conducted in 53,475 patients between June 2009 and March 2018 at Memorial Sloan Kettering
66 Cancer Center (MSKCC) (**Fig. 1a**). ^{18}F-FDG PET/CT was conducted for cancer diagnosis,
67 staging, monitoring of treatment response, and surveillance, and it is protocol at MSKCC to
68 report on BAT status in each study. BAT was reported on 7,923 (5.7%) ^{18}F-FDG PET/CT scans
69 (**Fig. 1b, Extended Data Table 1**) in 5,070 (9.5%) patients (**Fig. 1c, Extended Data Table 2**),
70 consistent with prior studies[5,6,11,16]. To assess accuracy of reporting and our search strategy, all
71 scans conducted in 2016 with reported BAT were manually reviewed. Of the 1,139 scans that
72 reported brown fat in 2016, 1,132 (99.4%) PET scans showed increased ^{18}F-FDG uptake in
73 regions identified as fat on CT in typical locations (neck, supraclavicular, axillary, mediastinal,
74 paraspinal and abdominal) while 4 (0.4%) scans reported a possible signature and 3 (0.3%)
75 scans were false-positive since they reported resolution of previously reported brown fat. While

the usage of ^{18}F-FDG PET/CT increased over the years in this study, the prevalence of BAT reporting remained consistent (**Extended Data Fig. 1**).

Patients were categorized by the presence or absence of BAT, and for those with multiple scans an index scan was assigned (**Fig. 1a**, described in methods). Brown fat was more prevalent among women (13.6 vs. 4.8%, $P<0.0001$), decreased with age (r=-0.9842, $P<0.0001$), and was inversely correlated with ambient temperature (r=-0.7093, $P<0.0001$) and BMI (r=-0.4360, $P=0.0007$), in accord with prior smaller retrospective studies (**Fig. 1d-g and Extended Data Fig. 2a and b**)[10,11].

Propensity score matching (PSM) allows for pairing of subjects with and without brown fat, while accounting for covariates that predict the likelihood of having brown fat. We used PSM to generate a study cohort without brown fat (N = 5,070), matching the individuals with brown fat based on sex, age, BMI and outdoor temperature at the time of the index scan (**Fig. 1h**). This resulting study cohort was balanced across the aforementioned variables (**Tab. 1; Extended Data Fig. 3**).

Individuals with brown fat showed significantly lower prevalence of type II diabetes (4.6 vs. 9.1%, $P<0.0001$) and dyslipidemia (18.9 vs. 20.6%, $P=0.0318$). This protective effect was also seen for cardiovascular disease, including atrial fibrillation/flutter (2.8 vs. 3.7%, $P=0.0071$), coronary artery disease (3.1 vs. 5.0%, $P<0.0001$), cerebrovascular disease (2.1 vs. 3.1%, $P=0.0011$), congestive heart failure (1.0 vs. 2.1%, $P<0.0001$) and hypertension (26.7 vs. 29.6%, $P=0.0003$) (**Fig. 2a**).

Cancer-associated characteristics such as cachexia, cancer type and stage have previously been associated with differences in brown fat prevalence on ^{18}F-FDG PET/CT, as has the use of beta-blocker drugs[11,17,18,19]. These associations were also observed in our study (**Extended Data Table 3 and Table 1)**. We used logistic regression analysis, adjusted for cancer site, cancer stage, and beta-blocker use, and demographic variables (including race, ethnicity, smoking status) to determine whether brown fat independently correlated with

102 cardiometabolic disease. Multivariable logistic regression analysis identified brown fat as an
103 independent negative predictor of type II diabetes (OR=0.46; 95% CI=0.39-0.55; *P*<0.0001),
104 coronary artery disease (OR=0.63; 95% CI=0.50-0.79; *P*<0.0001), congestive heart failure
105 (OR=0.56; 95% CI=0.40-0.80; *P*=0.0012) and hypertension (OR= 0.88; 95% CI=0.79-0.97;
106 *P*=0.0130) (**Fig. 2b and Extended Data Table 4**).

107 Next, we stratified these data by BMI to determine whether the association between
108 brown fat and improved cardiometabolic health was retained in overweight and obese
109 individuals. As the prevalence of metabolic and cardiovascular disease increased with higher
110 BMI, this effect was mitigated in individuals with brown fat (**Fig. 2c**). The benefit associated with
111 brown fat was most striking for type II diabetes and coronary artery disease. For example, the
112 prevalence of type II diabetes in individuals with BMI > 30 kg/m^2 and brown fat was less than
113 half of the prevalence in obese individuals without brown fat (7.5 vs. 19.1%, *P*<0.0001).
114 Significantly lower prevalences of hypertension (39.9 vs. 47.0%, *P*=0.0020) and congestive
115 heart failure (1.1 vs. 2.9%, *P*=0.0060) were also observed in individuals with obesity and brown
116 fat. Using the multivariable logistic regression model described above, we confirmed that brown
117 fat was independently associated with the observed decrease in cardiometabolic disease
118 prevalence in obese individuals (**Fig 2c**).

119 Next, we analyzed available laboratory values in temporal vicinity to the index scan to
120 further characterize the metabolic profile of the cohort. We noted distinct improvements in
121 glucose (91.7 vs. 95.1 mg/dl, *P*<0.0001), triglycerides (122.4 vs. 148.4 mg/dl, *P*=0.0006), and
122 HDL levels (56.4 vs. 52.2 mg/dl, *P*=0.0001) in individuals with brown fat, while there were no
123 differences for LDL (112.1 vs. 110.3 mg/dl, *P*=0.4406) and total cholesterol (192.3 vs. 188.6
124 mg/dl, *P*=0.1492) (**Fig. 2d and Extended Data Table 5**). By stratifying laboratory values by
125 BMI, we found that changes in fasting blood glucose and triglycerides associated with elevated
126 BMI were offset in individuals with brown fat, and HDL levels were higher across all BMI
127 categories in individuals with brown fat (**Fig. 2d**). There were no apparent differences in

128 laboratory values measuring renal function (creatinine 0.83 vs. 0.84 mg/dl, *P*=0.4537 and blood
129 urea nitrogen 14.6 vs. 14.8 mg/dl, *P*=0.1532) and thyroid function (TSH 2.95 vs. 2.49 mIU/L,
130 *P*=0.1764) (**Extended Data Table 5**). However, both leukocyte (6.2 vs. 6.8 10^9 cells/L,
131 *P*<0.0001) and platelet counts (250 vs. 260 10^9 cells/L, *P*=0.0007) were significantly decreased
132 in subjects with brown fat, suggesting potential roles for brown adipose beyond direct regulation
133 of lipid and glucose metabolism (**Extended Data Table 5**). In summary, our data support an
134 important role for brown fat in mitigating metabolic disease and its cardiovascular sequelae,
135 particularly in obese individuals.

136 Thermogenic fat promotes energy expenditure, and there is increasing evidence that this
137 tissue plays roles in metabolism beyond thermogenesis itself[20,21,22]. While thermogenesis clearly
138 modulates glucose and lipid metabolism, an association between thermogenic fat and blood
139 pressure has not been described until now. Furthermore, transcriptomic profiling indicates that
140 murine beige fat, as opposed to developmentally pre-formed brown fat, closely approximates
141 the inducible brown fat detected by PET/CT in adult humans[23]. We therefore used adipocyte-
142 specific PRDM16 knockout (Adipo-PRDM16 KO) mice (**Extended Data Fig. 4a, b, and c**) with
143 an ablation of beige fat function to investigate the potential link between thermogenic fat and
144 blood pressure control[24]. Interestingly, a previous genome-wide association study demonstrated
145 an association between a coding SNP in exon 9 of PRDM16 (leading to the missense mutation
146 Pro633Leu) and hypertension in humans[25].

147 Adipo-PRDM16 KO animals were implanted with radiotelemetric devices to monitor
148 blood pressure over a three-week period (**Fig. 3a**). Our studies were conducted in 11 to 14-
149 week-old mice on a standard chow diet, and body weight was equivalent between genotypes
150 throughout the study (**Extended Data Fig. 4d)**. Significant increases in systolic (difference
151 between means 3.6 mmHg; 95% CI 0.9-6.4, *P*=0.0102), diastolic (difference between means
152 4.2 mmHg; 95% CI 1.2-7.2, *P*=0.0071), mean arterial blood pressure (difference between
153 means 4.0 mmHg; 95% CI 1.8–6.3, *P*=0.0007) and heart rate (difference between means 18

154 bpm, 95% CI 3-33, *P*=0.0202) were apparent in KO animals versus controls (**Fig. 3a and**
155 **Extended Data Table 6**). After adjustment for heart rate, genotype remained independently
156 associated with increased systolic (difference between means 2.8 mmHg; 95% CI 0.2–5.5,
157 *P*=0.0378), diastolic (difference between means 3.3 mmHg; 95% CI 0.4–6.2, *P*=0.0281) and
158 mean arterial blood pressure (difference between means 3.3 mmHg; 95% CI 1.0–5.6,
159 P=0.0052) (**Extended Data Table. 7**).
160 There were no significant differences in heart weight, wall thickness, cardiac function or cardiac
161 tissue histology, indicating that neither cardiac morphology nor function were responsible for the
162 observed differences in systemic blood pressure (**Fig. 3b and Extended Data Fig. 5a**). We thus
163 explored resistance vasculature morphology and function. By using the pressure myograph
164 system, second order mesenteric arteries isolated from Adipo-PRDM16 KO mice (after
165 dissecting off all perivascular fat) demonstrated an increased contractile response specifically to
166 angiotensin II, with no significant differences in response to acetylcholine or phenylephrine (**Fig.**
167 **3c**). Additionally, vasodilation in response to a stepwise increase in flow was significantly
168 decreased in Adipo-PRDM16 KO mice while myogenic tone induced by a stepwise increase in
169 pressure did not show a difference between the genotypes (**Extended Data Fig. 5b)**.
170 Histological analysis evidenced no apparent structural differences (**Fig. 3d**). There were no
171 significant differences in plasma levels of angiotensinogen (**Fig. 3e**) or expression of
172 angiotensin receptors in the mesenteric arteries (**Fig. 3f**). In summary, ablation of beige fat
173 function in mice leads to an increased sensitivity of resistance arteries to angiotensin II,
174 contributing to elevated systemic blood pressure.

175 Obesity is a major contributor to metabolic and cardiovascular disease, and 48.9% of
176 American adults are predicted to be obese by 2030[26]. With limited effective therapies available,
177 thermogenic fat has been implicated as a potential therapeutic target for obesity and metabolic
178 disease[27]. In healthy adults, cold stimulation of brown fat increases energy expenditure and
179 improves systemic glucose utilization, fatty acid oxidation, and insulin sensitivity[28,29,30,31]. This
180 observation is consistent with animal models, where transplantation of thermogenic adipose
181 tissue mass improved glucose and triglyceride metabolism, while genetic ablation of
182 thermogenic fat had the opposite effect[3,32,33]. The effects of thermogenic adipose tissue on
183 cardiometabolic health and obesity-associated diseases in humans, however, have been largely
184 unexplored until now.

185 Our study illustrates that individuals with thermogenic fat on ^{18}F-FDG PET/CT have
186 significantly improved metabolic profiles. This effect is not only limited to diabetes, but extends
187 to coronary artery disease, congestive heart failure and hypertension. Furthermore, the effects
188 of brown fat on metabolic and cardiovascular disease are most pronounced among individuals
189 with elevated BMI. While obesity is generally associated with decreased brown fat function[34],
190 those obese individuals who retain brown fat activity appear to be protected against conditions
191 linked to excess weight. This notion further supports the potential of brown fat as a therapeutic
192 target beyond weight loss itself, but as a means to uncouple obesity from disease.

193 The reduction in the prevalence of hypertension associated with thermogenic fat was of
194 particular interest to us, because this cannot be directly explained by improvements in glucose
195 and lipid metabolism. Our studies in a mouse model lacking beige fat identified changes in
196 sensitivity to angiotensin II in the peripheral resistance vasculature as a potential underlying
197 physiological mechanism. Thermogenic fat secretes a number of endocrine factors that can
198 affect a wide variety of tissues, and ongoing research is focused on elucidating the downstream
199 effectors of these signals. Our work points towards a novel molecular signal linking adipose

200 tissue phenotype to blood pressure control, and may be the first step in elucidating a
201 mechanistic link between brown fat and hypertension.

202 Our study raises a number of questions regarding brown fat development and function in
203 humans. Variability in brown fat prevalence and activity suggests a possible genetic determinant
204 of its biology. Consistent with this, our understanding of genetics as a contributor to type II
205 diabetes development has evolved significantly[35]. It is likely then that genetic factors
206 contributing to brown fat development and activity may affect the pathogenesis of type II
207 diabetes and metabolic syndrome. In our study, brown fat was associated with improved health
208 across several organ systems. As an example, individuals without brown fat exhibited higher
209 leukocyte counts, and elevated white blood cell counts are an established risk factor for
210 coronary artery disease[36,37,38]. Decreased leukocyte counts in individuals with brown fat could, in
211 part, explain the lower prevalence of coronary artery disease among these subjects. Our work
212 highlights the need to determine the extent of brown fat's effects on other organs and roles in
213 systemic metabolism.

214 The major strength of our study is the size of the dataset, the largest we are aware of,
215 and the linkage to electronic health records. This allowed us to comprehensively examine
216 associations between brown fat and a wide variety of data. There are, however, a number of
217 limitations that need to be acknowledged, mainly pertaining to the retrospective design and
218 analysis of data from a cancer population. First, identification of brown fat relies on ^{18}F-FDG
219 PET/CT and consistent reporting. Our manual review of brown fat reporting over an entire year,
220 as well as a consistent brown fat prevalence over the study period, support the reliability of
221 reporting in this study. Furthermore, ^{18}F-FDG PET/CT without prior cold stimulation tends to
222 underestimate brown fat prevalence, which may have impacted our classification. In the
223 absence of broadly applicable screening methods or biomarkers for brown fat, the application of
224 ^{18}F-FDG PET/CT to screen for brown fat is however still considered the gold standard. Although
225 a number of studies have indicated associations between cancer characteristics and brown fat

226 prevalence as measured by ^{18}F-FDG PET/CT, the effect of cancer is still poorly understood. We
227 have thus adjusted our analysis to accommodate the potential influence of cancer type and
228 stage.

229 In our study, we investigated and confirmed new clinical findings linking thermogenic
230 adipose tissue and improvements in metabolic health using an established mouse model. These
231 findings will have the potential to enable translation of animal findings into viable human
232 therapies. Our study highlights the therapeutic potential of modulating brown fat in humans to
233 combat the escalating obesity crisis.

234

Online Methods

Study Design and Participants

This retrospective case-control study followed institutional guidelines and was approved by the Institutional Review Boards of The Rockefeller University and Memorial Sloan Kettering Cancer Center (MSKCC). Due to the retrospective nature of this study, the requirement for informed consent was waived. Results from this study are reported in accordance with the Strengthening the Reporting of Observational Studies in Epidemiology (STROBE) guidelines for case-control studies[39].

We identified all patients age 18 and above who underwent ^{18}F-FDG PET/CT at MSKCC from June 2009 through March 2018. This resulted in 139,224 ^{18}F-FDG PET/CT scans conducted in 53,475 patients. Brown adipose is identified by increased ^{18}F-FDG uptake on PET, measured in regions corresponding to adipose tissue on CT, and it is standard practice at MSKCC to document these signatures in all reports. We searched all ^{18}F-FDG PET/CT reports for the terms “brown fat” or “brown adipose”. Patients were then categorized by the presence or absence of brown fat reporting. For each subject in both groups, an index scan was designated as follows: in patients with brown adipose tissue reported on at least one ^{18}F-FDG PET/CT scan, the first scan that reported brown fat was defined as the index scan. In patients without brown fat on any scan, the first ^{18}F-FDG PET/CT scan served as the index scan (**Fig. 1**).

Data collection

We obtained average outdoor temperatures in New York City, measured in Central Park, for the months of scans from the U.S. National Weather Service. All patient data including demographics and self-reported race and ethnicity were collected from institutional electronic health records (EHR). Diagnoses listed up to one year after the time (month and year) of the index scan were identified using diagnostic codes from the International Classification of Diseases, 9th and 10th Revisions (ICD-9 and ICD-10) (**Supplementary Data Table 1**).

261 Laboratory values were recorded from the EHR if these values were first measured within three
262 months (complete blood counts) or one year (lipid levels) of the index scan date. In case of
263 multiple data points available, the one closest to the index scan was used for analysis. Blood
264 glucose was routinely measured on the day of scanning. Complete blood counts from patients
265 with hematological malignancies were excluded from analysis. With the exception of fasting
266 blood glucose, measurement of blood values was not coupled to ^{18}F-FDG PET/CT scans. Data
267 completeness was assessed for all blood values, and available data was analyzed using
268 complete case analysis (**Extended Data Table 5**). Data completeness ranged from 11.7% (low-
269 density lipoproteins) to 98.1% (glucose).
270

271 **Propensity Score Matching and Identification of Study Cohort**

272 To identify the study cohort, patients with reported brown fat were matched to patients without
273 reported brown fat using propensity score matching. Propensity scores were estimated using a
274 non-parsimonious multivariable logistic-regression model with brown adipose tissue status
275 (presence or absence) as the dependent variable and age, sex, BMI, and temperature at time of
276 scan as covariates. Matching was performed using a 1:1 protocol without replacement (greedy-
277 matching algorithm), a caliper width of 0.2 and the variable sex was set to be exactly matched.
278 We used standardized difference means to assess balance before and after matching
279 (**Extended Data Fig. 3**). Matching was conducted in SAS version 9.4 (SAS Institute, Cary, NC)
280 using the **psmatch** function.
281

282 **Outcomes**

283 ICD-9/10 diagnoses extracted from EHRs were used to examine associations between brown
284 fat and cardiometabolic health defined as the prevalence of type II diabetes, dyslipidemia,
285 hypertension, coronary artery disease, congestive heart failure and cerebrovascular disease. All
286 ICD-9/10 codes used to assign disease categories are listed in **Supplementary Data Table 1**.

287

288 **Data Analysis**

289 We first assessed the correlation between brown fat and age, outdoor temperature in the month
290 of the ^{18}F-FDG PET/CT index scan and BMI. For age and BMI, a one-phase exponential decay
291 curve was modeled and the correlation was assessed by calculating Spearman's rank
292 correlation coefficient. For temperature, a linear regression line was calculated and the
293 correlation was assessed by calculating Spearman's rank correlation coefficient. Prevalence of
294 brown fat in men and women was compared using chi-squared test. Brown adipose status
295 (either present or absent) and prevalence of cardiometabolic diseases were compared using
296 chi-squared tests.

297 Next, we assessed whether brown fat status was an independent predictor of cardiovascular
298 disease by using multivariable logistic regression analysis. The dependent variable in this
299 analysis was the respective cardiometabolic disease and brown fat status (presence or
300 absence) was the independent variable. To adjust for potential confounders that were selected
301 based on previous publications, we controlled for the following variables: age, sex, BMI, outdoor
302 temperature in Central Park in the month of the index scan, smoking status, race, ethnicity,
303 family history of cardiovascular disease, beta blocker use, cancer site, and cancer stage.

304 Smoking was coded as a categorical variable with 4 levels (current smoker, previous smoker,
305 never smoker, unknown smoking status). Race was a categorical variable with 4 levels:
306 Caucasian, African-American, Asian and other (e.g. Pacific-Islanders, unknown). Ethnicity was a
307 categorical variable with three levels: Hispanic, Non-Hispanic and Unknown. Cancer stage was
308 a 6 level categorical variable consisting of Stages I-IV, not applicable (e.g. hematologic
309 malignancies, benign tumors), and unknown cancer stage. Cancer site was recorded according
310 to ICD 0 Site Codes and included 14 categories: C00-C14, C15-C26, C30-C39, C40-C41, C42,

311 C43-C44, C45-C49, C50-C58, C60-C63, C64-C68, C69-C72, C73-C75, C76-C80 and
312 other/unknown. Results were reported as odds ratio and 95% confidence interval.
313 Cardiometabolic diseases that were independently associated with brown fat status were further
314 stratified by BMI categories (normal weight, defined as BMI <25km/m^2; overweight, defined as
315 BMI 25.0 – 30.0 kg/m^2; obese, defined as BMI >30.0 kg/m^2). Comparison between individuals
316 with and without brown fat in the respective category were performed using the multivariable
317 logistic expression model outlined above to assess whether observed differences were
318 statistically significant. For the comparison of laboratory values, a Student's *t*-test was
319 performed. To compare associations between brown fat status, BMI and available lab values, a
320 least squares linear regression line was constructed, stratified by brown status. All p-values are
321 two-tailed, and values less than 0.05 were considered statistically significant.

322

323 **Animal Experiments**

324 Animal care and experimentation were performed according to procedures approved by the
325 Institutional Animal Care and Use Committee at the Rockefeller University. The Adipo-PRDM16
326 KO mice were generated by breeding Prdm16lox/lox mice with Adiponectin-cre mice (provided
327 by Dr. Evan Rosen, backcrossed to a C57BL/6J background)[24]. Mice were maintained in 12 hr
328 light:dark cycles at 23C and fed a standard irradiated rodent chow diet.

329

330 **RNA Preparation and Quantitative PCR**

331 Total RNA was extracted from adipose tissue using TRIzol (Cat # 15596018, Thermo Fisher
332 Scientific, Waltham, MA, USA) along with RNeasy mini kits (Cat # 74104, QIAGEN, Venlo,
333 Netherlands). For qPCR analysis, RNA was reverse transcribed using the ABI high capacity
334 cDNA synthesis kit (Cat # 4368813, Thermo Fisher Scientific, Waltham, MA, USA). cDNA was
335 used in qPCR reactions containing SYBR-green fluorescent dye (Cat # 4309155, Thermo Fisher
336 Scientific, Waltham, MA, USA). Relative mRNA expression was determined by normalization

with Eukaryotic 18S ribosomal RNA levels using the DDCt method. Primer sequences are listed in **Supplementary Data Table 2.**

Implantation of Radiotelemetry Devices and Blood Pressure Measurement

Blood pressure was measured by implantable radio transmitters as previously described[40]. Briefly, male mice at age 11-14 weeks were housed in pairs. Prior to implantation, the animals received buprenorphine (0.8 mg/Kg, s.c.) and a transmitter was implanted (model HD-X11, Data Sciences International, St. Paul, MN, USA), while mice were under isoflurane anaesthesia. The catheter tip was positioned in the thoracic aorta via the left common carotid artery and the body of the probe was inserted subcutaneously in the dorsal right flank. Animals were allowed to recover for 5–7 days. Heart rate (HR), systolic blood pressure (SBP), diastolic blood pressure (DBP), and mean arterial pressure (MAP) were collected weekly over a 24h period in freely moving conscious mice in their cages. Pressure traces were checked and animals with damping of the haemodynamic profile were excluded from the analysis

Analysis of Blood Pressure Readings

For each mouse, systolic, diastolic and mean arterial blood pressure as well as heart rate was recorded. The mean for each parameter was calculated over a 24h period. Data from 4 experiments were pooled and used for the final analysis. A linear mixed model for repeated measures over time (SAS Proc Mixed) was used to analyze the radiotelemetry data with fixed effects of genotype (KO vs. WT), week treated as a categorical factor, and the interaction between genotype and week. This method prevented list-wise deletion due to missing data. Unstructured covariance structure was chosen with the lowest corrected Akaike's information criteria and Bayesian information criteria. Heart rate was included as a covariate for the blood pressure models and the adjusted mean difference between KO and WT mice with 95 % confidence intervals were reported.

363

364 **Mass Spectrometry**

365 12 µl of serum sample were incubated with 12 µL of 20mM dithiothreitol (DTT) and 16 M urea
366 (final 8M urea, 10 mM DTT, 50mM ammonium bicarbonate (ABC)) for 1h at room temperature
367 (RT). Another 6 µL of 50mM DTT were added to the samples (in 50 mM ABC, no urea) to
368 ensure complete reduction. The samples were then alkylated by addition of 20 µL of 75mM
369 iodoacetamide (IAA; 30mM final in ABC) in the dark at RT for 1.5h. 6 µg of LysC was added to
370 each of the sample. The samples were then allowed to digest at 28° C overnight with shaking.
371 The following day, the samples were further diluted with 60 µL of 50mM ABC. 10 µg of trypsin
372 was added to each of the samples and samples were digested with trypsin for 6 hours at 28° C
373 at 1400 rpm. The samples were then quenched with 10 µL of 10% TFA (pH approximately 1). 5
374 µL of sample was loaded onto 4 C18 empore discs. The cleaned up samples were speed
375 vacuumed and re-dissolved in 20 µL of 0.1% LC-grade formic acid. 1 uL was loaded onto a
376 reverse-phase nano-LC-MS/MS (EasyLC 1200, Fusion Lumos, Thermo Fisher Scientific) for
377 analysis. Peptides were separated with a gradient in which the proportion of buffer B (H2O with
378 0.1% formic acid) in buffer A (acetonitrile with 0.1% formic acid) increased from 2% to 90% over
379 79 minutes (300 nl/min flow rate). MS and MS/MS data were recorded at resolutions of 60.000
380 and 30.000 with AGC's of 1,000,000 and 50,000 respectively. Parallel reaction monitoring
381 (PRM) was used to target peptides unique to AGT
382 (AIQGLLVTQGGSSSQTPLLQSIVVGLFTAPGFR and LPTLLGAEANLNNIGDTNPR). PRM
383 experiment data were analyzed with SkyLine v.4.2. Samples were analyzed in the following
384 order: KO, WT and values were normalized to WT to derive fold-change between the two
385 genotypes.

386

387

388

389 **Tissue Staining**

390 Mesenteric arteries and hearts were collected from 18-week-old male mice. Briefly, mice were
391 euthanized by isoflurane overdose and the mesenteric artery was isolated and perfused with 50
392 mmol/L PBS (pH 7.4) followed by 4% PFA. After fixation overnight, tissues were washed 3x with
393 PBS and stored in ethanol 70%. Further tissue processing was performed at the Memorial
394 Sloan Kettering Cancer Center (MSKCC) Laboratory of Comparative Pathology. Briefly, the
395 tissues were embedded in paraffin and the dewaxed slides were first immersed in Weigert's
396 hematoxylin (Sigma, St. Louis, MO, U.S.A.), followed by serial staining with acid fuschin,
397 phosphomolybdic acid and methyl blue. The tissues were then fixed in 1% acetic acid. After
398 dehydration with increasing concentrations of alcohol, the slides were fixed in toluene, mounted
399 in Permount and air-dried overnight before acquiring photographs.

400

401 **Echocardiography**

402 Mice were anaesthetized with isoflurane under continuous monitoring and placed on a heating
403 pad of a recording stage connected to a Vevo 2100 ultrasound machine. The anterior chest wall
404 was shaved, ultrasound gel was applied and electrodes were connected to each limb to
405 simultaneously record an electrocardiogram. Two-dimensional (short axis-guided) M-mode and
406 B-mode measurements (at the level of the papillary muscles) were taken using an 18–32 MHz
407 MS400. For analysis, at least three measurements were averaged; measurements within the
408 same HR interval (450 ± 50 bpm) were used for analysis.

409

410 ***Pressure myography***

411 Mesenteric arteries were collected from 18-week-old male mice, as described above. Second
412 order mesenteric arteries (MA) were cleaned of surrounding fat and vascular reactivity
413 experiments were performed as described previously [41]. Briefly, MA were mounted on glass
414 cannulas in a pressure myograph chamber (Danish MyoTechnology, Aarhus, Denmark) The

vessel orientation in relation to the flow *in vivo* was maintained. Vessel viability was maintained using Krebs solution solution (in mM: NaCl 118, KCl 4.7, $MgCl_2$ 1.2, KH_2PO_4 1.2, $CaCl_2$ 2.5, $NaHCO_3$ 25 and glucose 10.1), at 37 °C and oxygenated (95% O_2 and 5% CO_2). A pressure interface controlled intraluminal pressure and flow in MA. The vessel diameter was monitored in real time using a microscope connected to a digital video camera (IC Capture) and computer software VediView 1.2 (Danish MyoTechnology, Aarhus, Denmark) with edge detection capability. MA were equilibrated for 15 min at 80 mm Hg, pre-constricted with PE (1 μM) and a cumulative concentration-response curve of Ach (0.1 nM – 30 μM) was performed to evaluate the integrity and the function of the endothelium. MA with less than 80% vasodilatory response to Ach were discarded. Vascular smooth muscle functions were evaluated by performing cumulative concentration-response curves of PE (1 nM – 30 μM), AngII (0.1 nM – 1 μM) and myogenic tone. Flow mediated vasodilation was also evaluated as previously described [41].

Statistical Analysis

Unless otherwise stated, data are presented as mean ± s.e.m. and are derived from multiple experiments. Normality was assessed using the Shapiro-Wilk-test. No statistical method was used to calculate sample size, but sample size was determined based on preliminary experiments and previous publications. Analysis was carried out using unpaired Student's *t*-test, Mann-Whitney U test or two-way ANOVA based on data distribution and as indicated. All p-values are two-tailed, and values less than 0.05 were considered statistically significant. GraphPad Prism 8 was used for statistical analysis.

Acknowledgements

We thank Dr. Robin Davisson for guidance on establishing radiotelemetric blood pressure monitoring, Michael N. Singer and Chester Poon for expert IT support and data extraction, Rebecca Teng for assistance in accessing data, and Dr. Barry S. Coller, Dr. Andrew J. Dannenberg, Dr. Javid J. Moslehi and Melissa D. Curtis for valuable discussions during the preparation of this manuscript.

Author Contributions

P.C. and T.B. designed and conceived the study. T.B., D.J.K, S.J.M., A.G.W., I.D.G., S.D.B. and H.S. acquired data and performed experiments. P.C., T.B., S.P., R.V., C.S.J., A.M. and A.D.L. analyzed and interpreted the data. T.B, D.J.K. and P.C. wrote the manuscript with input from all authors.

Competing Interest Statement

All authors declare no competing interests.

Data Availability

Source data for figures 1, 2, 3 as well as extended data figure 1, 2, 4 and 5 are provided with the paper. All other data that support the findings of this study are available from the corresponding author upon reasonable request.

Source of Funding

T.B. was supported in part by the National Center for Advancing Translational Sciences, NIH, through Rockefeller University (Grant #UL1TR001866).

D.J.K. was supported by a Medical Scientist Training Program grant from the National Institute of General Medical Sciences of the National Institutes of Health under award number

T32GM007739 to the Weill Cornell/Rockefeller/Sloan Kettering Tri-Institutional MD-PhD Program and by a National Defense Science and Engineering Graduate Fellowship from the Office of Naval Research and the United States Department of Defense under award number ND-BIO-024-093.

P.C. was supported by the Sinsheimer Foundation.

A.D.L. was supported by National Heart, Lung, and Blood Institute of the National Institutes of Health grant R01 HL126913 and National Institute of Neurological Disorders and Stroke of National Institutes of Health grant R21 NS104512.

I.D.G was supported by the Austrian Marshall Plan Scholarship.

472 **References**

473 1. Rosen, E.D. & Spiegelman, B.M. What we talk about when we talk about fat. *Cell* **156**,
474 20-44 (2014).
475 2. Bartelt, A.*, et al.* Brown adipose tissue activity controls triglyceride clearance. *Nat. Med.*
476 **17**, 200-205 (2011).
477 3. Lowell, B.B.*, et al.* Development of obesity in transgenic mice after genetic ablation of
478 brown adipose tissue. *Nature* **366**, 740-742 (1993).
479 4. Cohen, P. & Spiegelman, B.M. Brown and Beige Fat: Molecular Parts of a Thermogenic
480 Machine. *Diabetes* **64**, 2346-2351 (2015).
481 5. Yeung, H.W.*, et al.* Patterns of (18)F-FDG uptake in adipose tissue and muscle: a
482 potential source of false-positives for PET. *J. Nucl. Med.* **44**, 1789-1796 (2003).
483 6. Cohade, C., Osman, M., Pannu, H.K. & Wahl, R.L. Uptake in supraclavicular area fat
484 ("USA-Fat"): description on 18F-FDG PET/CT. *J. Nucl. Med.* **44**, 170-176 (2003).
485 7. van Marken Lichtenbelt, W.D.*, et al.* Cold-activated brown adipose tissue in healthy men.
486 *N. Engl. J. Med.* **360**, 1500-1508 (2009).
487 8. Virtanen, K.A.*, et al.* Functional brown adipose tissue in healthy adults. *N. Engl. J. Med.*
488 **360**, 1518-1525 (2009).
489 9. Cypess, A.M.*, et al.* Identification and importance of brown adipose tissue in adult
490 humans. *N. Engl. J. Med.* **360**, 1509-1517 (2009).
491 10. Cronin, C.G.*, et al.* Brown fat at PET/CT: correlation with patient characteristics.
492 *Radiology* **263**, 836-842 (2012).
493 11. Steinberg, J.D., Vogel, W. & Vegt, E. Factors influencing brown fat activation in FDG
494 PET/CT: a retrospective analysis of 15,000+ cases. *Br. J. Radiol.* **90**, 20170093 (2017).
495 12. Brendle, C.*, et al.* Correlation of Brown Adipose Tissue with Other Body Fat
496 Compartments and Patient Characteristics: A Retrospective Analysis in a Large Patient
497 Cohort Using PET/CT. *Acad. Radiol.* **25**, 102-110 (2018).

498 13. Ouellet, V., *et al.* Brown adipose tissue oxidative metabolism contributes to energy
499 expenditure during acute cold exposure in humans. *J. Clin. Invest.* **122**, 545-552 (2012).
500 14. Yoneshiro, T., *et al.* Brown adipose tissue, whole-body energy expenditure, and
501 thermogenesis in healthy adult men. *Obesity (Silver Spring)* **19**, 13-16 (2011).
502 15. Orava, J., *et al.* Different metabolic responses of human brown adipose tissue to
503 activation by cold and insulin. *Cell Metab.* **14**, 272-279 (2011).
504 16. Cohade, C., Mourtzikos, K.A. & Wahl, R.L. "USA-Fat": prevalence is related to ambient
505 outdoor temperature-evaluation with 18F-FDG PET/CT. *J. Nucl. Med.* **44**, 1267-1270
506 (2003).
507 17. Kir, S. & Spiegelman, B.M. Cachexia & Brown Fat: A Burning Issue in Cancer. *Trends in*
508 *cancer* **2**, 461-463 (2016).
509 18. Cao, Q., *et al.* A pilot study of FDG PET/CT detects a link between brown adipose tissue
510 and breast cancer. *BMC Cancer* **14**, 126 (2014).
511 19. Fujii, T., *et al.* Implication of atypical supraclavicular F18-fluorodeoxyglucose uptake in
512 patients with breast cancer: Association between brown adipose tissue and breast
513 cancer. *Oncology letters* **14**, 7025-7030 (2017).
514 20. Villarroya, F., Cereijo, R., Villarroya, J. & Giralt, M. Brown adipose tissue as a secretory
515 organ. *Nat Rev Endocrinol* **13**, 26-35 (2017).
516 21. Choi, C.H.J. & Cohen, P. Adipose crosstalk with other cell types in health and disease.
517 *Exp. Cell Res.* **360**, 6-11 (2017).
518 22. Wang, G.X., Zhao, X.Y. & Lin, J.D. The brown fat secretome: metabolic functions
519 beyond thermogenesis. *Trends Endocrinol Metab* **26**, 231-237 (2015).
520 23. Shinoda, K., *et al.* Genetic and functional characterization of clonally derived adult
521 human brown adipocytes. *Nat. Med.* **21**, 389-394 (2015).
522 24. Cohen, P., *et al.* Ablation of PRDM16 and beige adipose causes metabolic dysfunction
523 and a subcutaneous to visceral fat switch. *Cell* **156**, 304-316 (2014).

524 25. Liu, C., *et al.* Meta-analysis identifies common and rare variants influencing blood
525 pressure and overlapping with metabolic trait loci. *Nat. Genet.* **48**, 1162-1170 (2016).
526 26. Ward, Z.J., *et al.* Projected U.S. State-Level Prevalence of Adult Obesity and Severe
527 Obesity. *N. Engl. J. Med.* **381**, 2440-2450 (2019).
528 27. Cypess, A.M. & Kahn, C.R. Brown fat as a therapy for obesity and diabetes. *Curr Opin*
529 *Endocrinol Diabetes Obes* **17**, 143-149 (2010).
530 28. Blondin, D.P., *et al.* Dietary fatty acid metabolism of brown adipose tissue in cold-
531 acclimated men. *Nat Commun* **8**, 14146 (2017).
532 29. Chondronikola, M., *et al.* Brown Adipose Tissue Activation Is Linked to Distinct Systemic
533 Effects on Lipid Metabolism in Humans. *Cell Metab.* **23**, 1200-1206 (2016).
534 30. Yoneshiro, T., *et al.* Recruited brown adipose tissue as an antiobesity agent in humans.
535 *J. Clin. Invest.* **123**, 3404-3408 (2013).
536 31. Hanssen, M.J., *et al.* Short-term cold acclimation improves insulin sensitivity in patients
537 with type 2 diabetes mellitus. *Nat. Med.* **21**, 863-865 (2015).
538 32. Liu, X., *et al.* Brown adipose tissue transplantation improves whole-body energy
539 metabolism. *Cell Res.* **23**, 851-854 (2013).
540 33. Feldmann, H.M., Golozoubova, V., Cannon, B. & Nedergaard, J. UCP1 ablation induces
541 obesity and abolishes diet-induced thermogenesis in mice exempt from thermal stress
542 by living at thermoneutrality. *Cell Metab.* **9**, 203-209 (2009).
543 34. Alcala, M., *et al.* Mechanisms of Impaired Brown Adipose Tissue Recruitment in Obesity.
544 *Front Physiol* **10**, 94 (2019).
545 35. Langenberg, C. & Lotta, L.A. Genomic insights into the causes of type 2 diabetes.
546 *Lancet* **391**, 2463-2474 (2018).
547 36. Yarnell, J.W., *et al.* Fibrinogen, viscosity, and white blood cell count are major risk
548 factors for ischemic heart disease. The Caerphilly and Speedwell collaborative heart
549 disease studies. *Circulation* **83**, 836-844 (1991).

550 37. Friedman, G.D., Klatsky, A.L. & Siegelaub, A.B. The leukocyte count as a predictor of
551 myocardial infarction. *N. Engl. J. Med.* **290**, 1275-1278 (1974).
552 38. Ensrud, K. & Grimm, R.H., Jr. The white blood cell count and risk for coronary heart
553 disease. *Am. Heart J.* **124**, 207-213 (1992).
554 39. von Elm, E.*, et al.* The Strengthening the Reporting of Observational Studies in
555 Epidemiology (STROBE) statement: guidelines for reporting observational studies.
556 *Lancet* **370**, 1453-1457 (2007).
557 40. McGavigan, A.K.*, et al.* Vertical sleeve gastrectomy reduces blood pressure and
558 hypothalamic endoplasmic reticulum stress in mice. *Disease models & mechanisms* **10**,
559 235-243 (2017).
560 41. Cantalupo, A.*, et al.* Nogo-B regulates endothelial sphingolipid homeostasis to control
561 vascular function and blood pressure. *Nat. Med.* **21**, 1028-1037 (2015).

562

563

564

565 **Fig. 1: a,** ^{18}F-FDG PET/CT reports were reviewed for reporting of brown adipose tissue
566 between June 2009 and March 2018 and individuals were stratified by presence or absence of
567 brown fat. An index scan was assigned and diagnosis codes and available laboratory values in
568 temporal vicinity were collected. **b**, Brown fat was reported in 5.7% of all ^{18}F-FDG PET/CT
569 scans (n=139,224). **c**, Brown fat was reported in 9.5% of all patients (n=53,475). **d**, Prevalence
570 of brown fat was higher in females compared with males. Groups were compared by chi-square
571 test, *P*-value is two-tailed. **e**, Brown fat prevalence was inversely correlated with age and
572 followed a one-phase decay. Spearman's rank correlation coefficient was calculated to assess
573 the correlation between brown fat prevalence and age, *P*-value is two-tailed. **f**, Brown fat
574 prevalence, based on ^{18}F-FDG PET/CT scans was inversely correlated with outdoor
575 temperature in the month of the scan between June 2009 and March 2018. Bars depict means,
576 error bars are s.e.m., dots are mean temperature for each year between 2009 and 2018. **g,**
577 Brown fat prevalence was inversely correlated with body mass index. **h**, Propensity score
578 matching was used to identify a matched cohort based on age, sex, body mass index and
579 outdoor temperature in the month of the index scan.

580

581 **Fig. 2: a,** Comparison of cardiometabolic disease prevalence between individuals with and
582 without brown adipose tissue (BAT). Groups were compared by chi-square test, all *P*-values are
583 two-sided. **b**, Forrest plots illustrate the association between brown fat status and
584 cardiometabolic disease in the propensity score matched cohort. Circles and bars represent
585 odds ratios (ORs) and 95% confidence intervals (CIs), respectively, and were calculated using
586 multivariable logistic regression analysis with adjustment for age, sex, body mass index, outdoor
587 temperature in the month of the index scan, ethnicity, race, smoking status, family history of
588 cardiovascular disease, beta blocker use, cancer site and cancer stage. All *P*-values are two

589 sided. Black circles and CI bars represent non-significant associations, red circles and CI bars
590 represent statistically significant associations at $P < 0.05$. **c**, Prevalence of cardiometabolic
591 disease stratified by brown status and body mass index using the WHO categories for normal
592 and underweight (body mass index (BMI) < 25.0 kg/m^2), overweight (BMI between 25.0 and
593 30.0 kg/m^2) and obesity (BMI > 30.0 kg/m^2). Patients per category: BMI < 25.0 kg/m^2, with
594 brown fat *n* = 2,564, without brown fat *n* = 2,639; BMI between 25.0 and 30.0 kg/m^2, with brown
595 fat *n* = 1,589, without brown fat *n* = 1,491; BMI > 30.0 kg/m^2, with brown fat *n* = 917, without
596 brown fat *n* = 940. Significance was assessed using multivariable logistic regression adjusted
597 for age, sex, body mass index, outdoor temperature in the month of the index scan, ethnicity,
598 race, smoking status, family history of cardiovascular disease, beta blocker use, cancer site and
599 cancer stage. *P* values are depicted for values <0.1. All *P* values are two sided. **d**, Comparison
600 of available laboratory values between matched individuals with and brown fat (glucose; with
601 brown fat n = 5,033 (99.3%), without brown fat n = 4,963 (97.9%); triglycerides; with brown fat n
602 = 732 (14.4%), without brown fat n = 734 (14.5%); high-density lipoprotein; with brown fat n =
603 596 (11.8%), without brown fat n= 578 (11.4%); low density lipoprotein; with brown fat n = 543
604 (10.7%), without brown fat n = 527 (10.4%); total cholesterol; with brown fat n = 637 (12.6%),
605 without brown fat n = 630 (12.4%). Groups were compared with Student's t-test, dots represent
606 means, error bars 95% confidence intervals, all *P*-values are two-sided. Values with statistically
607 significant differences were stratified by body mass index and a linear regression line for body
608 mass index values between 18.5 and 40.0 kg/m^2 was calculated. Shaded areas depict 95%
609 confidence intervals.

610

611 **Fig. 3: a,** Implanted radiotelemetery devices were used to measure systolic, diastolic and mean
612 arterial blood pressure and heart rate in freely moving mice with an adipocyte-specific knockout
613 (KO) of *Prdm16* or wildtype (WT) controls (n=35 per group from a total of 4 independent

experiments). Dots depict mean, error bars are s.e.m. A linear mixed model for repeated measures over time was used to analyze the radiotelemetry data with fixed effects of genotype (KO vs. WT), week treated as a categorical factor, and the interaction between genotype and week. [a] denotes *P*-values that were calculated by adjusting the above mentioned linear mixed model by heart rate to account for the observed differences in heart rate. All *P*-values are two-sided. **b**, Heart weight at necropsy normalized to body weight, ejection fraction and fractional shortening (both assessed by echocardiography) were measured in KO (n=12) and WT (n=8) animals. Bars represent means, error bars are s.d. Groups were compared by Student's t-test. All *P*-values are two-sided. **c** Pressure myography after removal of perivascular fat was conducted in KO and WT animals (n=3 per group; 2 mesenteric arteries per mouse) to assess response to acetylcholine (endothelium-dependent vasorelaxation), phenylephrine and angiotensin II (both vasoconstrictions). Dots represent means, error bars are s.e.m. Groups were compared by two-way analysis of variance (ANOVA). All *P*-values are two-sided. **d**, Mesenteric arteries were stained with Masson's trichrome stain to compare WT and KO animals. Representative image, n=5 per group. Scale bar is 50 μm. **e**, Angiotensinogen levels were measured in KO and WT animals using mass spectrometry (n = 8 per group). Groups were compared using Student's t-test. All *P*-values are two-sided. **f**, Expression of angiotensin receptors on mesenteric arteries was assessed using quantitative PCR (qPCR); n=5 per group. Groups were compared using Student's t-test. All *P*-values are two-sided.

Extended Data Fig. 1: a, The total number of ^{18}F-FDG PET/CT scans performed at MSKCC increased from 2009 to 2018 while the prevalence of reported brown fat remained stable. Dots depict total number of ^{18}F-FDG PET/CT scan in each year, half filled dots illustrate years with incomplete reporting. Bars represent prevalence of ^{18}F-FDG PET/CT scans with reported brown fat.

639

640 **Extended Data Fig. 2. a,** Correlation between body mass index and prevalence of brown fat
641 reported on ^{18}F-FDG PET/CT. The dotted line depicts a one-phase decay curve, *P*-value was
642 calculated for the correlation between both variables using Spearman's r. **b**, Correlation
643 between outside temperature in the month of the scan and prevalence of brown fat reported on
644 ^{18}F-FDG PET/CT. The dotted line depicts a linear regression line, *P*-value was calculated for the
645 correlation between both variables using Spearman's r. All *P*-values are two-sided.

646

647 **Extended Data Fig. 3.** Propensity score matching was assessed by comparing standardized
648 mean differences before and after the matching process. The blue shaded area indicates the
649 chosen caliper width.

650

651 **Extended Data Fig. 4. a**, The loxP sites flanking exon 9 and the adiponectin driven Cre-
652 recombinase that were used to create the *Prdm16* knockout (KO) mouse model are shown.
653 Radio telemetry devices to measure blood pressure were implanted in mice between the age of
654 11 and 14 weeks and measurements were started 1 week after implantation for 3 weeks.
655 Pressure myography and echocardiography were performed at the end of the study. **b**,
656 Expression of *Prdm16* in brown adipose tissue (BAT), subcutaneous adipose tissue (SQ) and
657 visceral adipose tissue (Visc) was measured by quantitative PCR (qPCR) and compared
658 between KO (n=8) and littermate control wildtype animals (WT; n=8). Groups were compared
659 using Mann-Whitney U test for non-normally distributed variables (BAT) and Student's t-test for
660 normally distributed variables (SQ and Visc). Bar depict means, error bars are s.e.m. All *P*-
661 values are two-sided. **c**, Expression of *Prdm16* in mesenteric arteries and adjacent mesenteric
662 adipose tissue was measured by quantitative PCR (qPCR) and compared between KO (n=4 for

663 mesenteric arteries' n=5 for mesenteric fat) and littermate control wildtype animals (WT; n=4 for
664 mesenteric arteries' n=5 for mesenteric fat). Groups were compared using Student's t-test. Bar
665 depict means, error bars are s.e.m. All *P*-values are two-sided. **d**, Comparison of body weights
666 between WT and KO animals (both n=35 at the beginning of the study). Groups were compared
667 using a mixed effects model with post-hoc analysis for individual time points.

668

669 **Extended Data Fig. 5. a**, Sections of the left ventricle were stained with Masson's trichrome
670 stain to compare fat specific *Prdm16* knockout (KO) and littermate control (wildtype; WT)
671 animals. Representative image, n=5 per group. Scale bar is 50 μm. **b**, Mesenteric arteries from
672 KO and WT were harvested, cleaned of perivascular fat and used for pressure myography (n=3
673 per group). Groups were compared using two-way analysis of variance (ANOVA). Dots
674 represent means, error bars s.e.m. All *P*-values are two-sided.

675

Table 1. Characteristics of Patients with and without Brown Fat Before and After Propensity Score Matching

Baseline Variable	Before Propensity Score Matching		After Propensity Score Matching		P-Value*
	Brown Adipose Present (BAT+) (N=5 070)	Brown Adipose Absent (BAT-) (N=48 405)	Brown Adipose Present (BAT+) After Matching (N=5 070)	Brown Adipose Absent (BAT-) After Matching (N=5 070)	
Age, mean (SD)	49.0 (16.3)	61.7 (14.0)	49.0 (16.3)	49.2 (15.8)	0.5863
Sex, No. (%)					
Women	3 879 (76.5)	24 711 (51.1)	3 879 (76.5)	3 879 (76.5)	1.0000
Men	1 191 (23.5)	23 694 (49.0)	1 191 (23.5)	1 191 (23.5)	
BMI, mean (SD)	25.8 (5.3)	27.8 (5.9)	25.8 (5.3)	25.6 (5.5)	0.0830
BMI category, No. (%)					
< 25.0	2,564 (50.6)	16,578 (34.3)	2,564 (50.6)	2,639 (52.1)	<0.0001
25.0 – 29.9	1,589 (31.3)	17,436 (36.0)	1,589 (31.3)	1,491 (29.4)	
> 30.0	917 (18.1)	14,391 (29.7)	917 (18.1)	940 (18.5)	
Race, No. (%)					
Asian	402 (7.9)	2 851 (5.9)	402 (7.9)	414 (8.2)	<0.0001
African American	561 (11.1)	3 396 (7.0)	561 (11.1)	434 (8.6)	
Caucasian	3 694 (72.9)	39 225 (81.0)	3 694 (72.9)	3 862 (76.2)	
Other or Unknown	413 (8.2)	2 933 (6.1)	413 (8.2)	360 (7.1)	
Ethnicity, No. (%)					
Hispanic	398 (7.9)	2 803 (5.8)	398 (7.9)	330 (6.5)	0.0281
Non-Hispanic	4 458 (87.9)	43 059 (89.0)	4 458 (87.9)	4 534 (89.4)	
Unknown	214 (4.2)	2 543 (5.3)	214 (4.2)	206 (4.1)	
Cardiovascular Risk Factors, No. (%)					
Family History of Cardiovascular Disease	1 029 (20.3)	11 714 (24.2)	1 029 (20.3)	1 086 (21.4)	0.1636
Smoking Status					
Current Smoker	513 (10.1)	5 390 (11.1)	513 (10.1)	588 (11.6)	<0.0001
Previous Smoker	1 169 (23.1)	17 755 (36.7)	1 169 (23.1)	1 261 (24.9)	
Never Smoker	2 999 (59.2)	19 923 (41.2)	2 999 (59.2)	2 654 (52.4)	
Unknown	389 (7.7)	5 337 (11.0)	389 (7.7)	567 (11.2)	
^{18}F-FDG PET/CT Characteristics					
Total Number of Scans per Patient, n (%)	4.1 (4.0)	2.5 (2.6)	4.1 (4.0)	2.5 (3.8)	<0.0001
Temperature (°C Month of Reference Scan), mean (SD)	11.9 (8.6)	13.6 (8.8)	11.9 (8.6)	12.0 (8.8)	0.7242
Beta blocker, n (%)	656 (12.9)	12 569 (26.0)	656 (12.9)	899 (17.7)	<0.0001

*P-value for the comparison of BAT+ and BAT- individuals in the propensity score matched group.

BAT, brown adipose tissue. SD, standard deviation. BMI, body mass index.

676

Fig. 1: Identification of brown fat and association with age, sex, body mass index and outdoor temperature. A propensity score matched cohort was constructed to adjust for differences in these individuals.

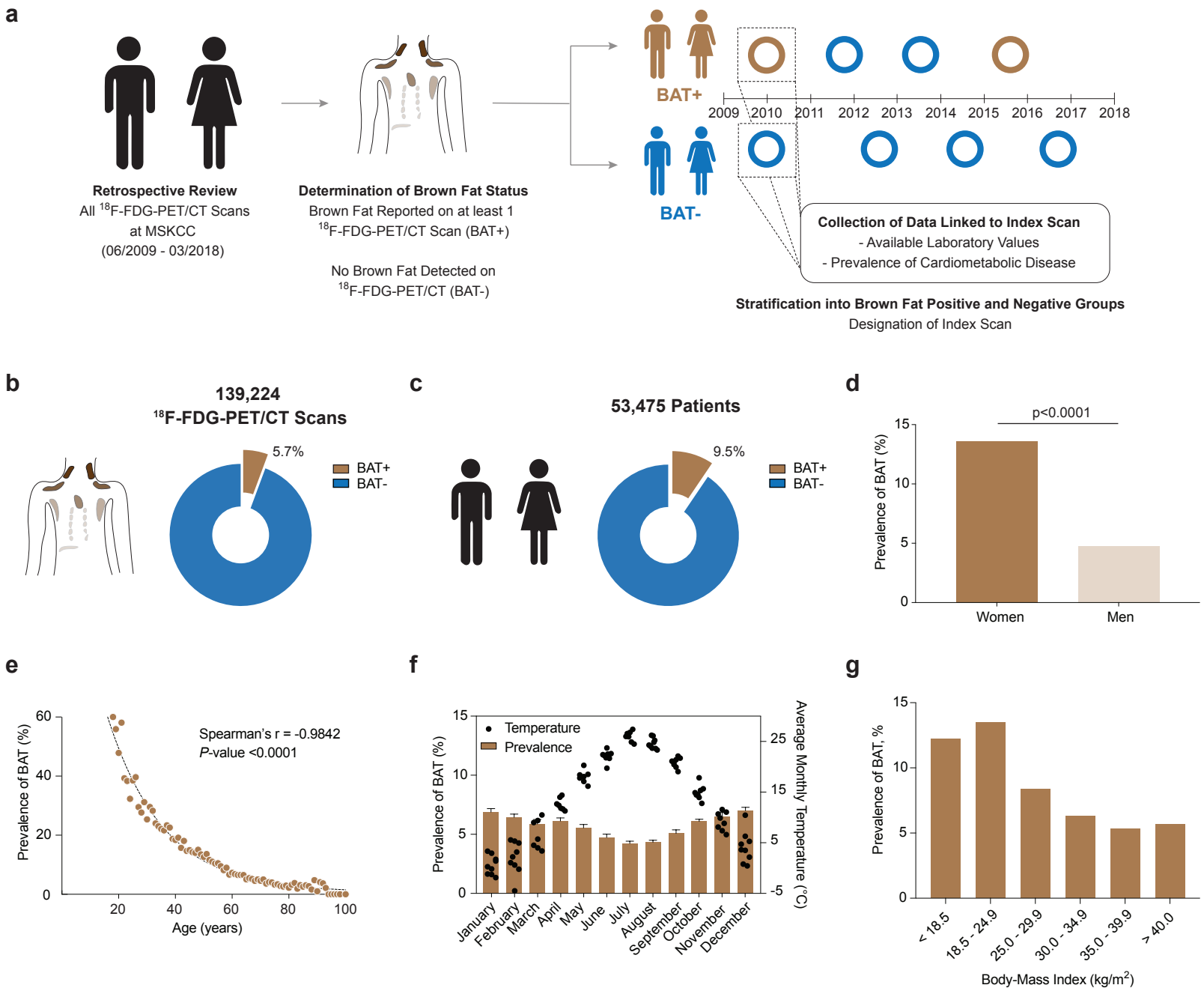

Fig. 2: Brown fat is associated with improved cardiometabolic health.

a

Diagnosis	BAT pos. (n = 5,070)	BAT neg. (n = 5,070)	P value
	n (%)	n (%)	
Type II diabetes	233 (4.6)	460 (9.1)	<0.0001
Dyslipidemia	956 (18.9)	1,042 (20.6)	0.0318
Atrial fibrillation/ Atrial flutter	140 (2.8)	188 (3.7)	0.0071
Coronary artery disease	159 (3.1)	254 (5.0)	<0.0001
Cerebrovascular disease	104 (2.1)	156 (3.1)	0.0011
Congestive heart failure	53 (1.0)	106 (2.1)	<0.0001
Hypertension	1,356 (26.7)	1,503 (29.6)	0.0003

b

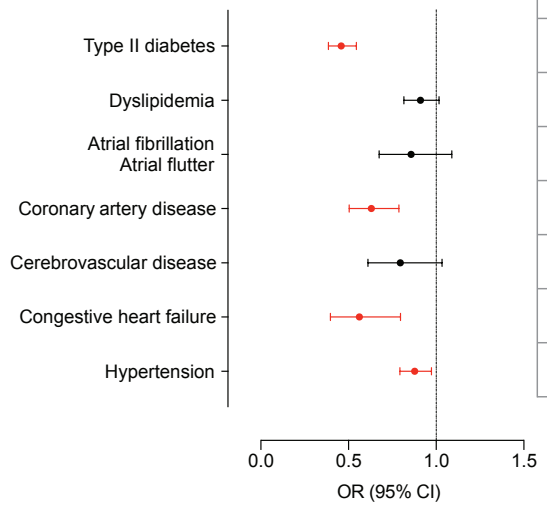

OR	95% CI	P value
0.46	0.39 - 0.55	<0.0001
0.91	0.82 - 1.02	0.0951
0.86	0.68 - 1.09	0.2081
0.63	0.50 - 0.79	<0.0001
0.80	0.61 - 1.03	0.0875
0.56	0.40 - 0.80	0.0012
0.88	0.79 - 0.97	0.0130

c

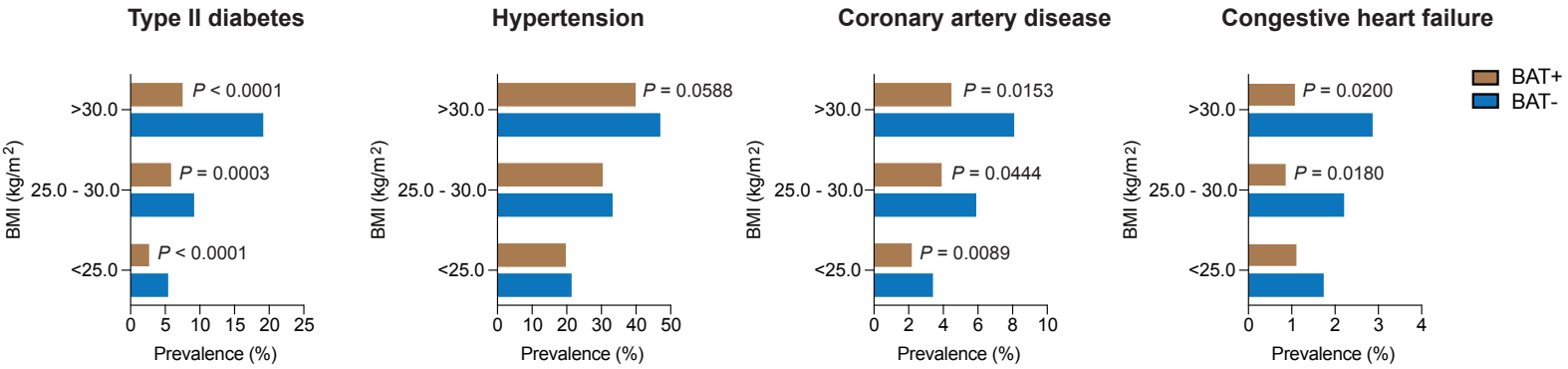

d

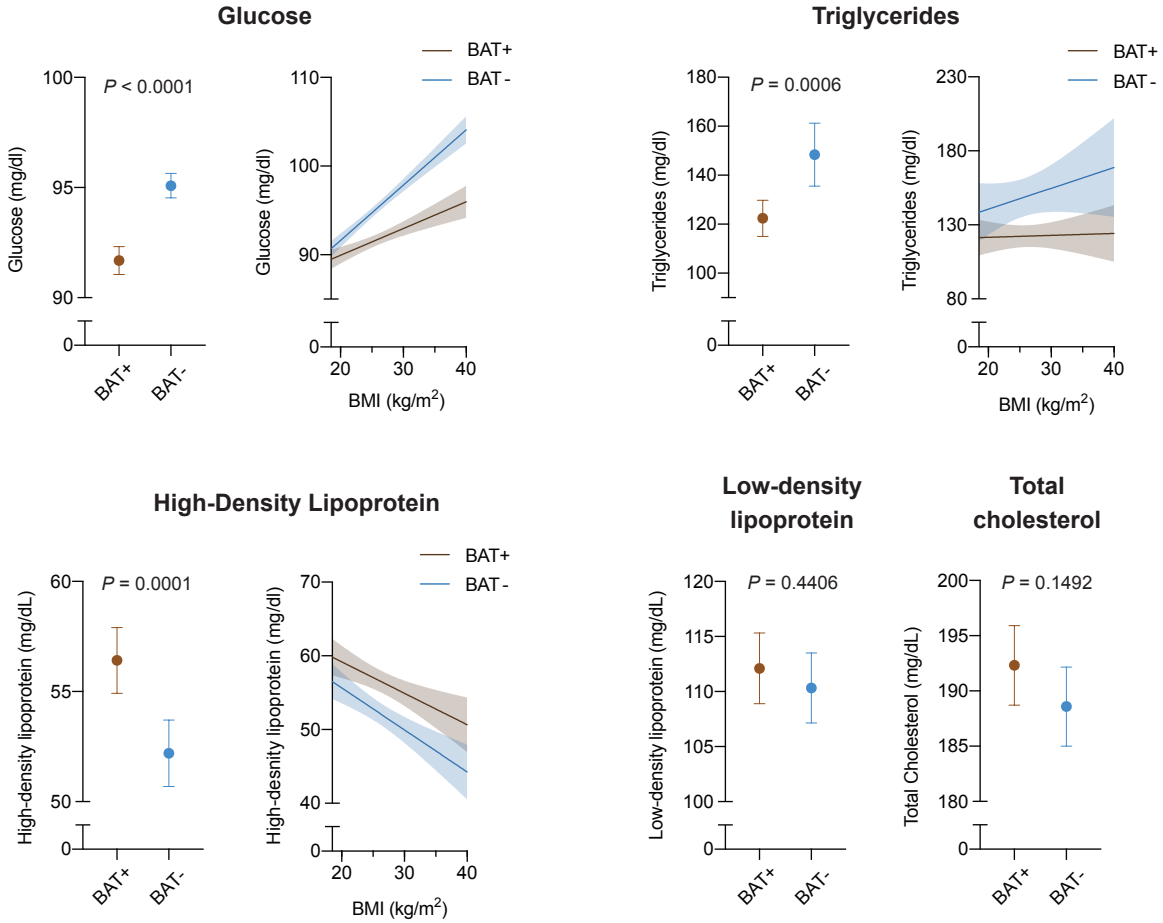

Fig 3. Ablation of thermogenic fat induces hypertension.

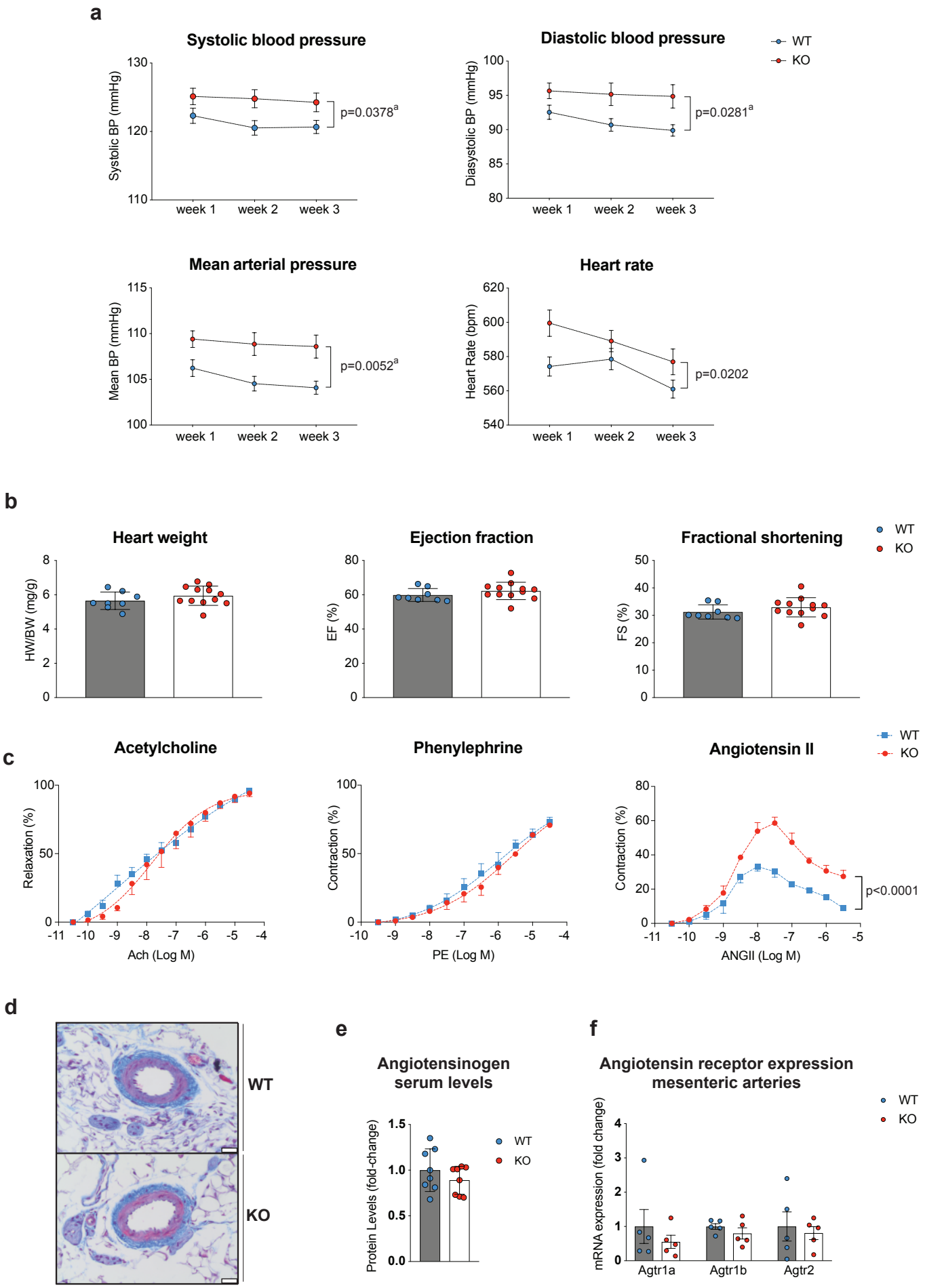

Extended Data Fig. 1: Number of ^{18}F-FDG PET/CT scans and brown fat prevalence between 06/2009 - 03/2018.

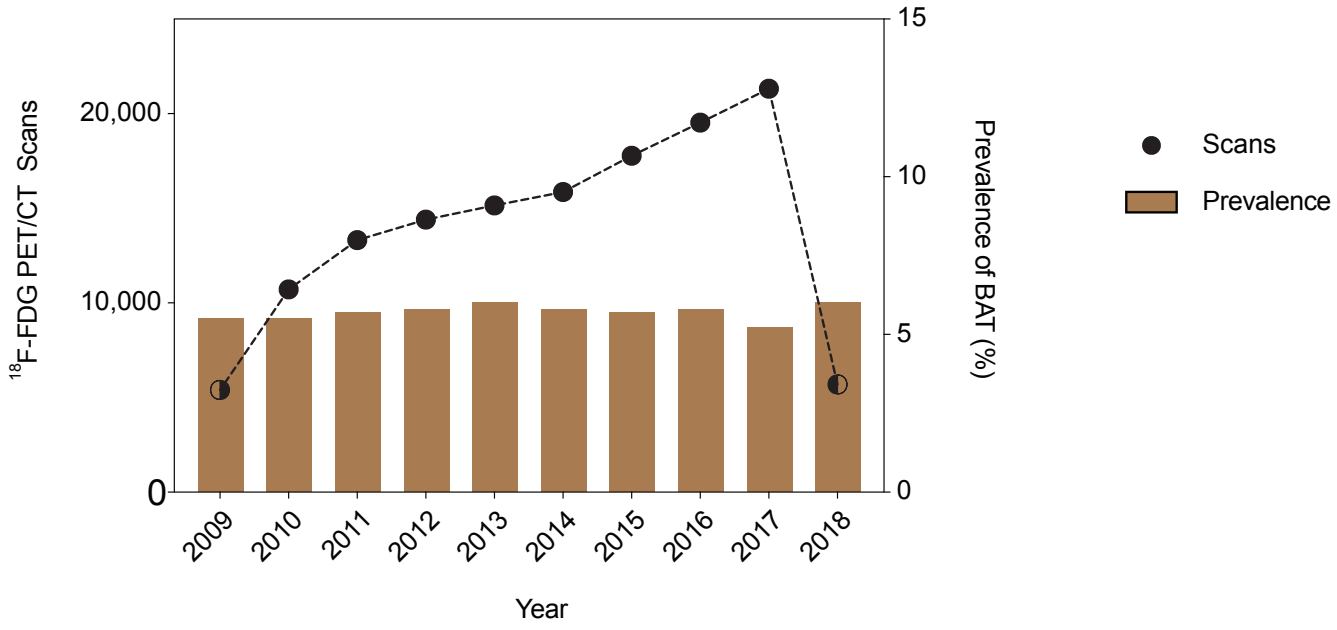

Extended Data Fig. 2: Correlation between brown fat prevalence and body mass index or outside temperature.

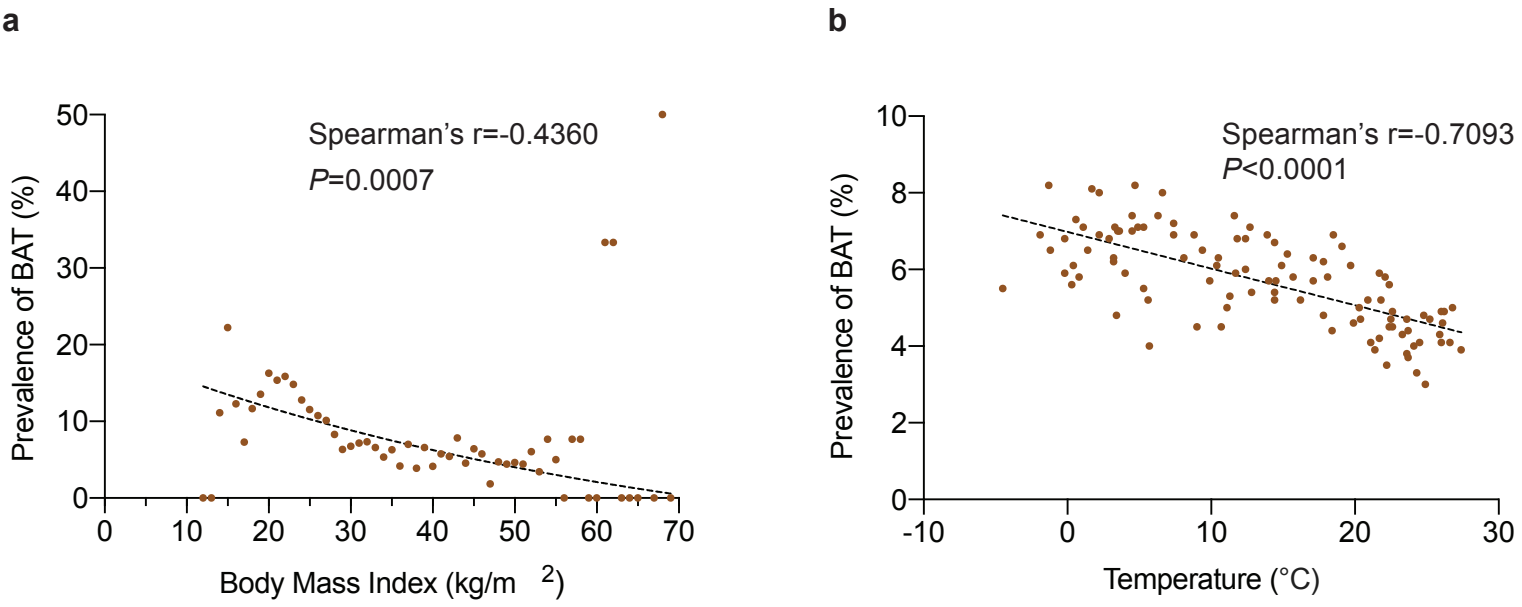

Extended Data Fig. 3: Standardized mean differences before and after propensity score matching.

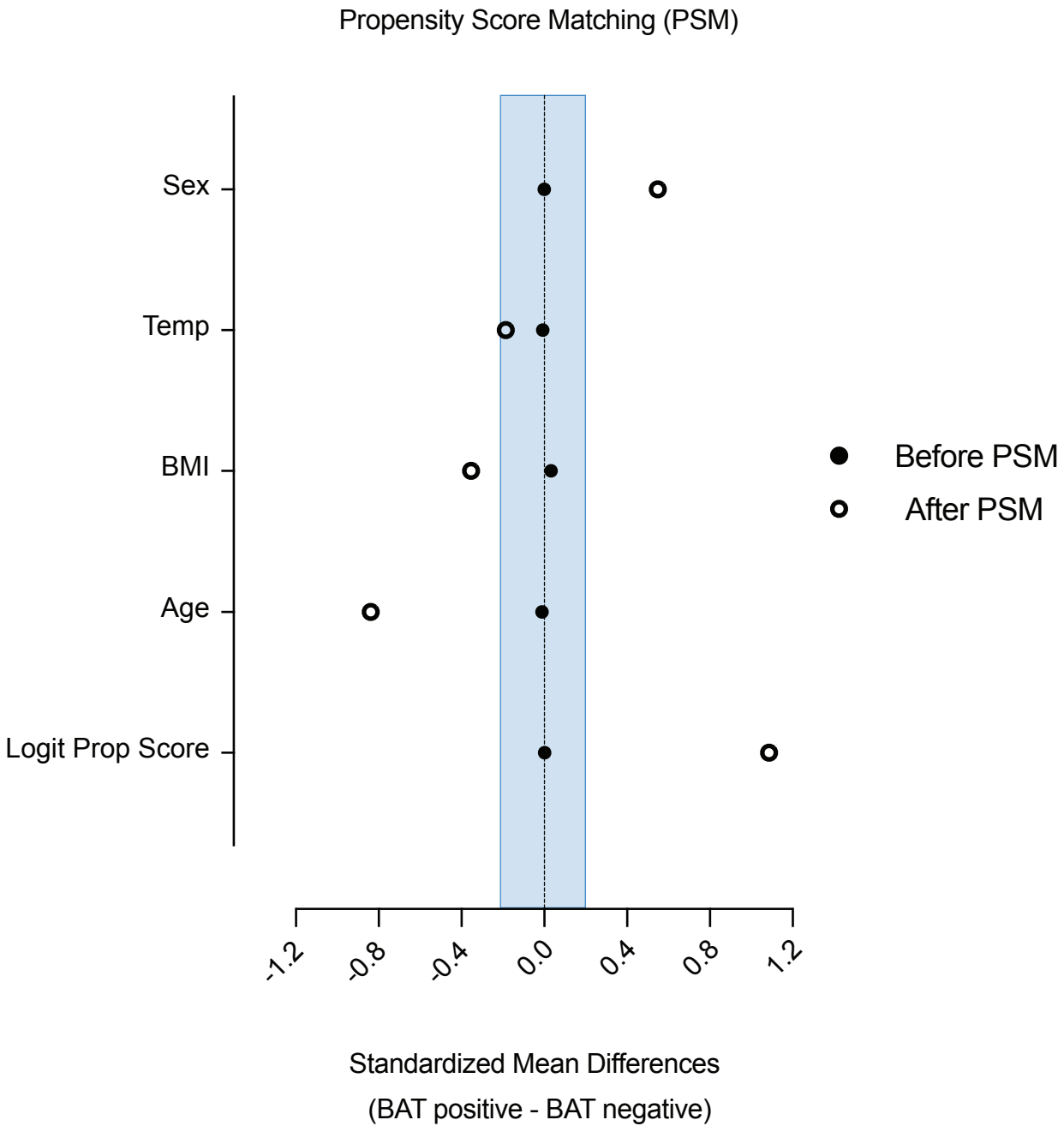

Extended Data Fig. 4: Study design and characteristics of the prdm16 mouse model.

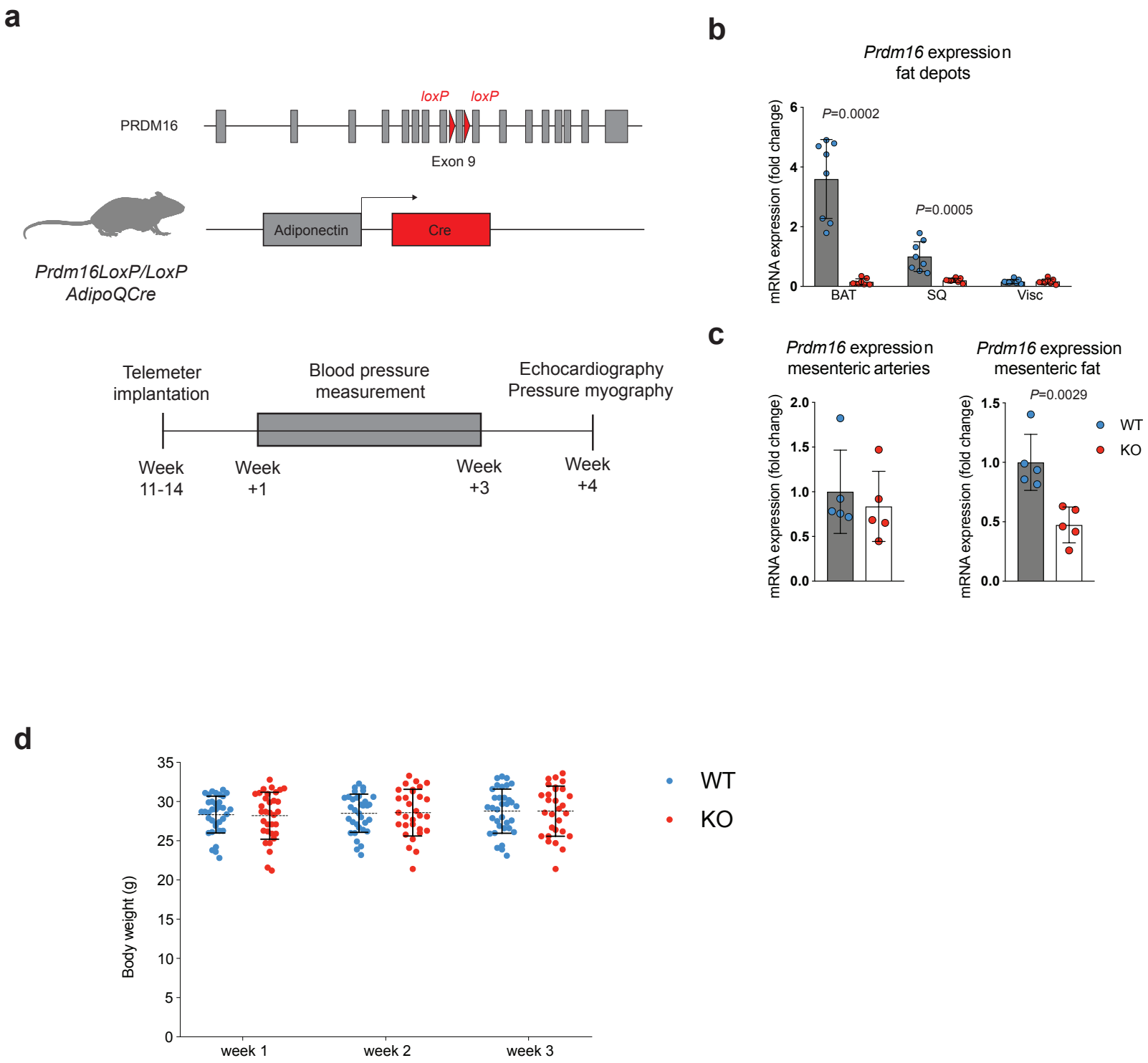

Extended Data Fig. 5: Cardiac histology and pressure myography.

a

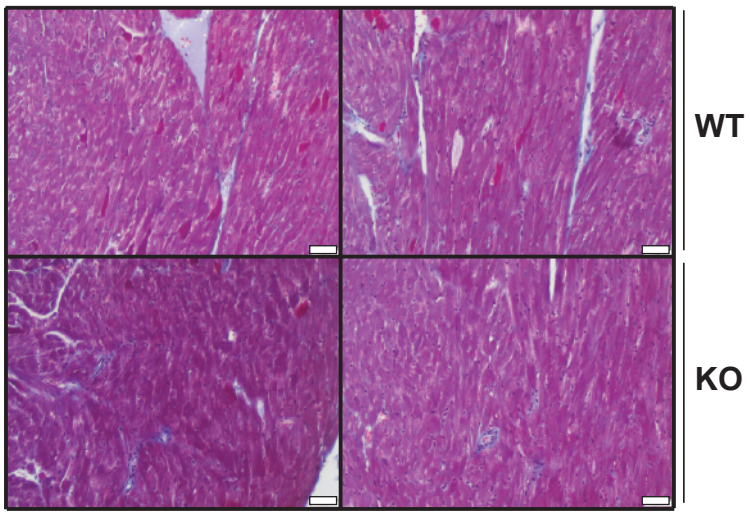
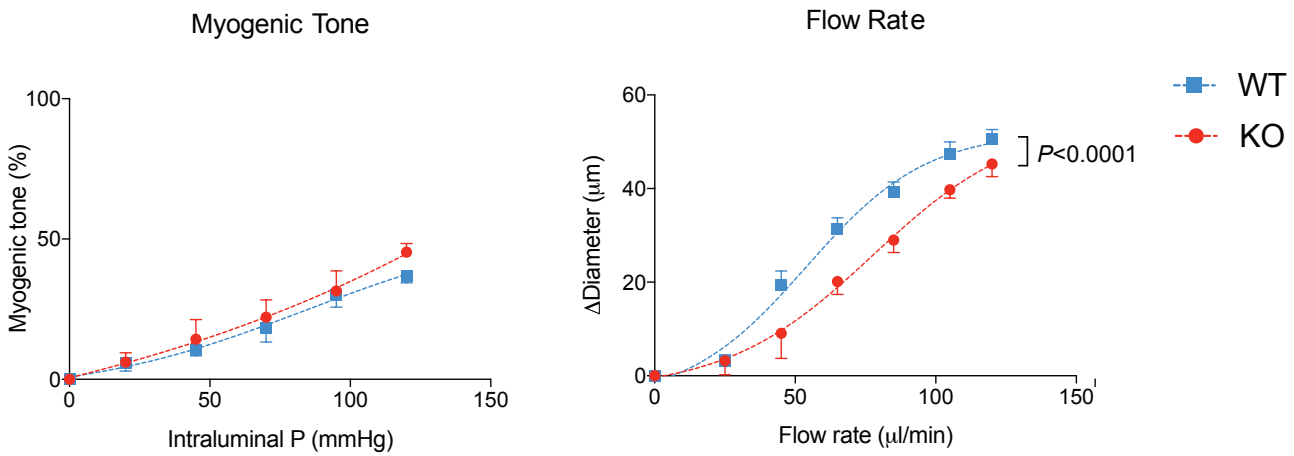
b